

Elastic considerations of field pull-out tests of polymer strip reinforcement

Takeharu Konami

R&D Division, Okasan Co., Ltd, Japan

Shigeyoshi Imaizumi & Satoru Takahashi

Utsunomiya University, Japan

ABSTRACT: A methodology by which frictional coefficient and rigidity were estimated using measurements of pull-out force at front end and tensile strain at any point along embedment length is presented based on theory of elasticity. Some results of field pull-out test are also shown. Analysis of field pull-out tests through proposed methodology shows that estimated frictional coefficients are little lower than those obtained through direct shear test and estimated rigidities are good agreement with those from tensile tests.

1 INTRODUCTION

Estimating a value of interface frictional coefficient between reinforcement material and soil is inevitable work for designing embedment length of strip reinforcement. Usually, direct shear tests or pull-out tests in laboratory have been conducted for this purpose (Koerner 1994). The pull-out test being conducted in the field, it often happens that the test has to stop before the reinforcement is perfectly pulled out because the elongation, i.e., deformation at front end, of material is so large as not to be measured. In such a case, a frictional coefficient can be estimated by knowing an effective area of interface. In order to know the area, engineers have to measure elongation at several points along embedment as conducted in laboratory pull-out test (Hayashi et. al 1994). This work, however, needs miscellaneous equipment including wires and guide tubes.

In this paper, a methodology by which frictional coefficient and rigidity (thickness times elastic modulus) can be estimated analyzing the measurements of pull-out force and displacement at front end of reinforcement embedded in ground and tensile strain at any points along embedment length is presented based on theory of elasticity. Field pull-out tests were also conducted for polymer strip which were used for vertical reinforced wall (Konami et. al 1992). The obtained data were analyzed through the proposed methodology to determine a frictional coefficient and rigidity.

2 ELASTIC FORMULA

Fig. 1 shows a basic model for strip geosynthetics embedded in soil and forces acting on it. The geosynthetic with elastic modulus of E has thickness

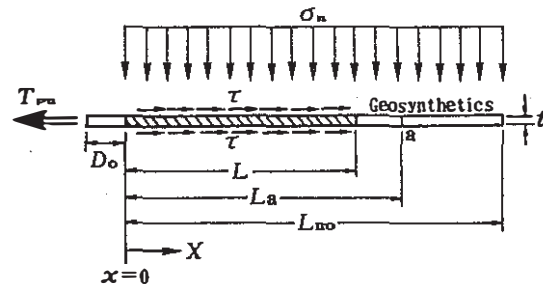


Fig. 1 Schematic drawing of pull-out test

of t and embedment length of L_{RO} . Uniformly distributed pressure σ_n acts on geosynthetic surface. It is assumed that the peak internal frictional coefficient μ can mobilize on both inter-surfaces between geosynthetics and soil immediately after relative displacement on interface occurs. This leads $\tau = \mu \cdot \sigma_n$. When pull-out force, T_{pu} , for unit width is applied to front end of geosynthetics, it will stretch over length of L . At a given point of $x < L$, the relationship between strain $\varepsilon(x)$, mobilized internal stress $\sigma(x)$ and infinitesimal deformation $ds(x)$ are;

$$\varepsilon(x) = \frac{\sigma(x)}{E} = \frac{ds(x)}{dx} \quad (1)$$

Equilibrium between internal tensile stress $\sigma(x)$ and pull-out force T_{pu} at front end is ;

$$\sigma(x) \cdot t = T_{pu} - \int_0^x \tau(x) ds$$

Table 1 Properties of reinforcements

Reinforcement Type	PW-3	PW-5	PW-10
Width b (cm)	8.5	9.0	9.0
Thickness t (cm)	0.2	0.3	0.5
Nominal Strength (kN)	29.4	49.0	98.1
Secant Rigidity $E \cdot t$ (kN/cm)	2%	34.3	53.9
	5%	23.0	39.2
		87.1	

$$= T_{pu} - 2 \cdot \mu \cdot \sigma_n \cdot x \quad (2)$$

Combining equations (1) and (2) gives;

$$ds(x) = \frac{1}{E \cdot t} (T_{pu} - 2 \cdot \mu \cdot \sigma_n \cdot x) dx \quad (3)$$

The elongation D_0 of geosynthetics at front end is obtained by integrating $ds(x)$ over a range of L .

$$D_0 = \int_0^L ds(x) = \frac{1}{E \cdot t} (T_{pu} \cdot L - \mu \cdot \sigma_n \cdot L^2) \quad (4)$$

As an element at $x = L$ has no strain, the stress $\sigma(L)$ is zero. This leads to the followings from equation (2).

$$L = \frac{T_{pu}}{2 \cdot \mu \cdot \sigma_n} \quad (5)$$

Combining equations (4) and (5), the elongation D_0 is expressed as ;

$$D_0 = \frac{1}{E \cdot t} \left\{ \frac{(T_{pu})^2}{2 \cdot \mu \cdot \sigma_n} - \frac{\mu \cdot \sigma_n \cdot (T_{pu})^2}{(2 \cdot \mu \cdot \sigma_n)^2} \right\} = \frac{(T_{pu})^2}{4 \cdot E \cdot t \cdot \mu \cdot \sigma_n} \quad (6)$$

Equation (6) shows that deformation at front end varies directly proportional to square of pull-out force and the coefficient α means rigidity ($E \cdot t$) times $4 \cdot \mu \cdot \sigma_n$.

Next, the stress at $x = L_a$ is presented as the followings from equation (2)

$$\sigma(L_a) \cdot t = T_{pu} - 2 \cdot \mu \cdot \sigma_n \cdot L_a \quad (7)$$

Substituting equation (7) into equation (1), we have

$$T_{pu} = \varepsilon(L_a) \cdot E \cdot t + 2 \cdot \mu \cdot \sigma_n \cdot L_a \quad (8)$$

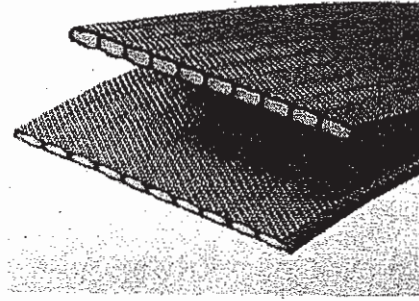


Fig. 2 Shape of polymer strip

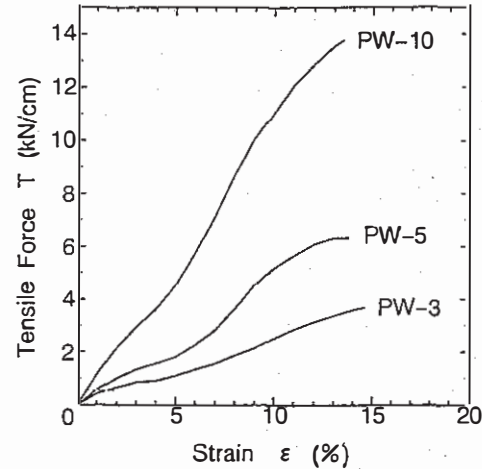


Fig. 3 Tensile force versus strain curves

This implies that the rigidity $E \cdot t$ of geosynthetics can be estimated as a gradient β of plots for pull-out force T_{pu} versus induced strain $\varepsilon(L_a)$ in geosynthetics at the position of $x = L_a$.

Considering α obtained previously, therefore, the frictional coefficient μ can be estimated as the followings.

$$\mu = \frac{\alpha}{4 \cdot E \cdot t \cdot \sigma_n} = \frac{\alpha}{4 \cdot \beta \cdot \sigma_n} \quad (9)$$

3 FIELD PULL-OUT TESTS

3.1 Properties of reinforcement and soil

Three types of polymer strip reinforcements, named *PW-3*, *PW-5* and *PW-10*, were used in the field pull-out tests. They are made up of the 8.5, 9.0 and 9.0 cm wide and 2, 3 and 5 mm thick, respectively, polyester fibers coated with polyethylene (see Fig. 2).

The properties of polymer strip reinforcement are shown in Table 1. Moreover the salient features such

Table 2 Conditions of embedded reinforcement

No.	1	2	3	4	5	6	7	8
Reinforcement Type	PW-5	PW-5	PW-3	PW-3	PW-10	PW-10	PW-5	PW-3
Embedment length (m)	3.5	3.5	3.5	3.5	5.5	5.5	5.5	5.5
Depth (m)	4.8	3.2	1.6	0.8	5.6	4.0	2.4	0.8

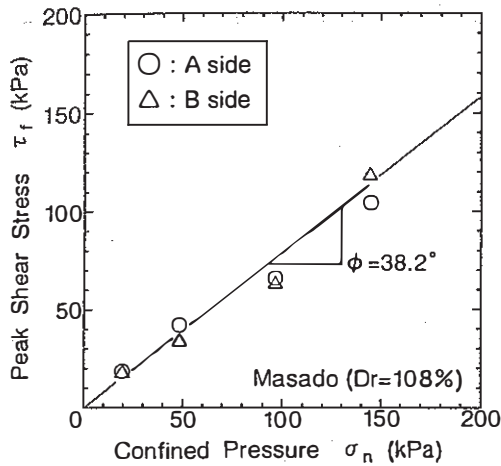


Fig. 4 Shear strength between reinforcement and soil

as the load-deformation characteristics from tensile test are shown in Fig. 3 for three kinds of materials. Their breaking due to tensile occurred with 14 % elongation approximately. On the other hand, 5 % elongation takes place under nearly 50 % load ratio against nominal strength. The secant rigidities at 2 % and 5% strain calculated from Fig. 3 are also listed in Table 1. The secant rigidities at 2% for PW-3, PW-5 and PW-10 are 34.3 kN/cm, 53.9 kN/cm and 102.3 kN/cm respectively.

The soil material used in tests is Masado (decomposite granite sandy soil) picked from Ubecity, Yamaguchi- prefecture. It has an optimum moisture content of $w_{opt} = 14.2\%$ and a dry density of $\gamma_d = 18.0 \text{ MN/m}^3$. The triaxial tests of the soil were conducted for the test sample with the degree of compaction of 90 % and resulted in internal friction angle of $\phi' = 37.2^\circ$.

The in-situ density of the sample of each layer after compaction was $\gamma_t = 20.6 \text{ MN/m}^3$ at natural condition and $\gamma_d = 18.6 \text{ MN/m}^3$ at dry condition on average. It was realized that the dry density in-situ was higher than that obtained in the laboratory.

3.2 Interface frictional resistance by direct shear test

Direct shear tests were conducted to estimate the interface frictional parameters between polymer material and Masado. It has upper shear box with a diameter of 60 mm and depth of 30 mm and a rigid bottom plate. Confined pressure was varied from 19.6 to 147.0 kPa. Fig. 4 shows the plots of peak

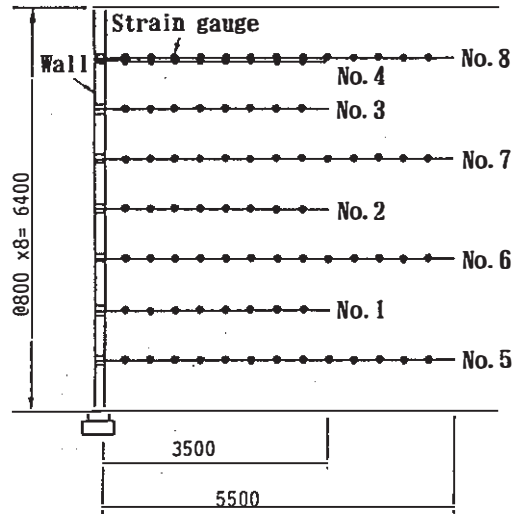


Fig. 5 Section of test embankment

shear stress versus confined pressure, from which frictional angle δ and cohesion c are determined to be 38.2° ($\mu = 0.787$) and 0 kPa respectively.

3.3 Specification of field pull-out test

The height of the test wall is 6.4 m and crest length is 12 m. The reinforcement laid in the backfill are shown in Fig. 5. The strain gauges were pasted on reinforcements at interval of 40 cm. The conditions of these reinforcements for pull-out are listed in Table 2. Pull-out force was applied to front end of reinforcement through center hole jack at a rate of 1 cm/min.

3.4 Pull-out tests results

Fig. 6 shows the relationships between pull-out force T_{pu} and displacement D_0 at front end of reinforcement that were obtained for the embedment length of 5.5 m. The displacement corresponding to same pull-out force seems to decrease with increasing an embedded depth of reinforcement. It also decreases with increasing of rigidity of material. These trends can be justified in quality based on equation (6). The pull-out forces, however, do not reach to their peak amount although the front end of reinforcement displaced up to 10 cm.

Figs. 7(a) to 7(c) show the distributions of tension strain creating in reinforcements due to

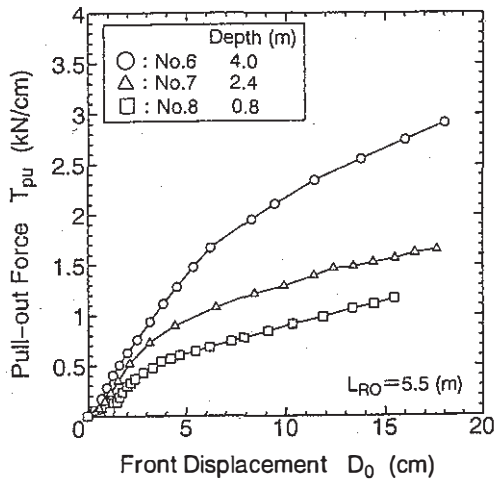


Fig. 6 Pull-out force versus displacement at front end

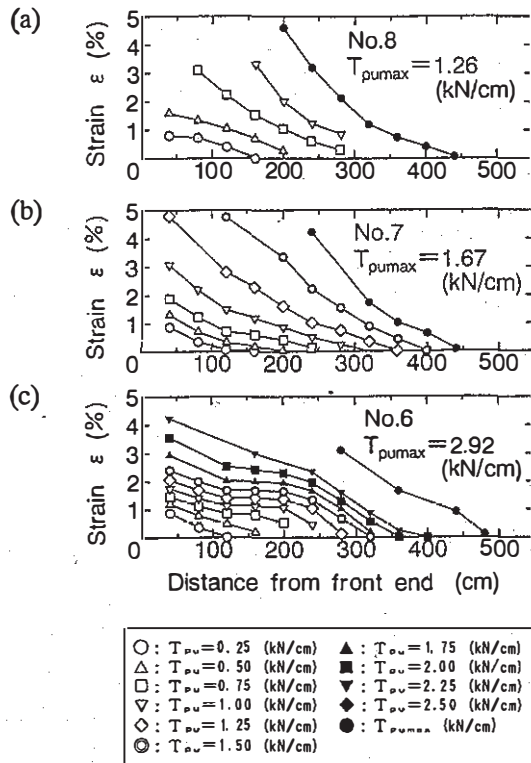


Fig. 7 Strain distribution in reinforcement

increased pull-out force. These figures indicate that tension strain created near the front end of reinforcement at lower pull-out force. As pull-out force increased, tensile strain progressed toward back end of reinforcement and the amount of it at given point increased. The strains that could create by higher pull-out force do not appear in the figures because the strain gauges were broken due to its large tension stress. This implies that the reinforcements were not pulled out perfectly and frictional resistance did not mobilize all over the embedment length.

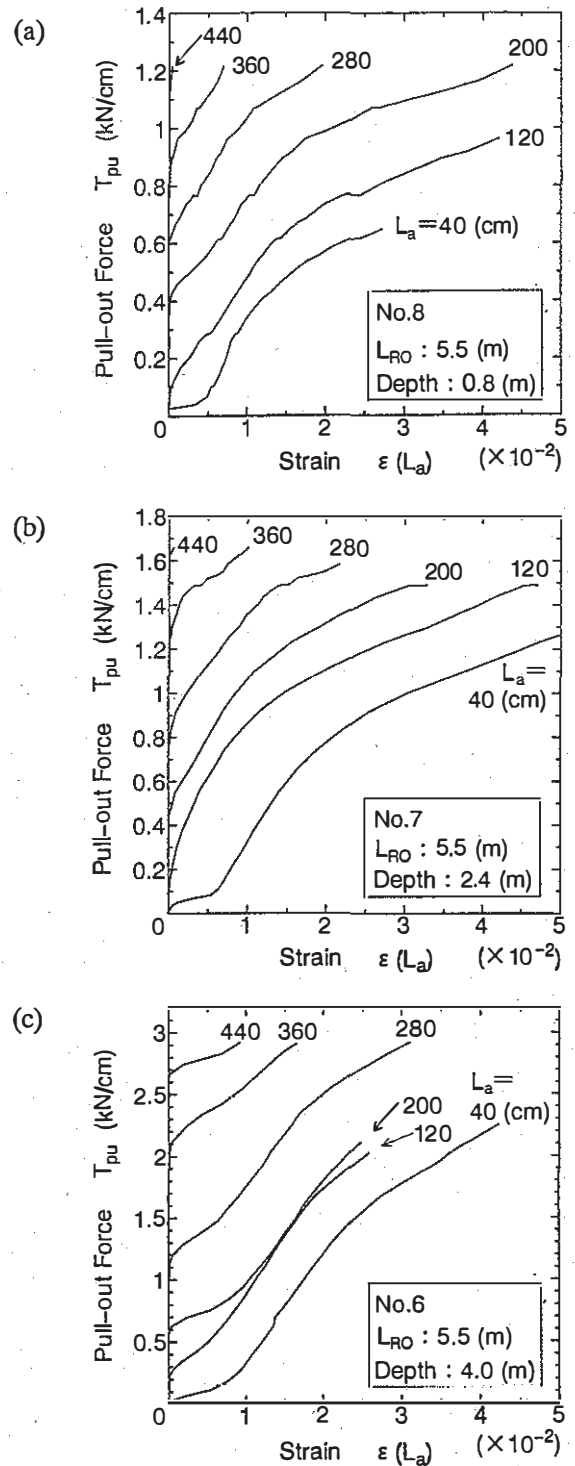


Fig. 8 Pull-out force versus strain at L_a

4 ESTIMATION OF FRICTIONAL COEFFICIENT AND RIGIDITY

Figs. 8(a) to 8(c) show the plots of pull-out force T_{pu} versus strain $\epsilon(L_a)$ creating at the position of $x = L_a$, where the amount of L_a took 40, 120, 200, 280, 360

Table 3 Estimated rigidities and frictional coefficients

Reinforcement Type	PW-3	PW-5	PW-10
Rigidity $E \cdot t$ (kN/cm)	38.8	59.7	80.3
Frictional Coefficient μ	0.409	0.200	0.246

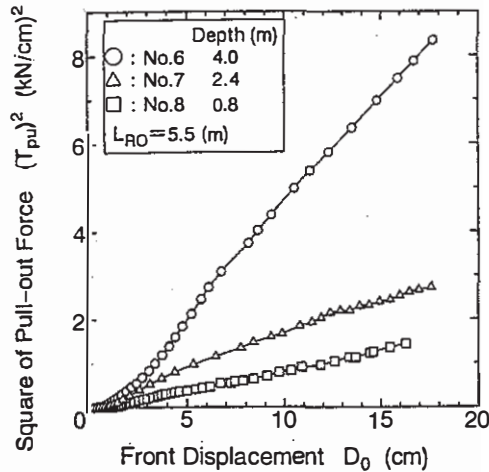


Fig. 9 Relationships between $(T_{pu})^2$ and D_0

and 440 cm. Though the relationships are not linear all over the strain, initial part looks as linear. Then the gradient β , which indicates an amount of rigidity $E \cdot t$ of reinforcement as mentioned previously, at strain less than 1.5 % was calculated from these Figures. It resulted in 34.1 to 43.1 with average of 38.8 kN/cm for $PW-3$, 46.0 to 70.4 with average of 59.7 kN/cm for $PW-5$ and 56.9 to 91.1 with average of 80.3 kN/cm for $PW-10$. These values are considered to be good agreement with secant rigidities at 2 % obtained from tensile tests.

Fig. 9 shows the plots of square of T_{pu} versus displacement D_0 at front end. It can be seen that square of T_{pu} varies approximately proportional to D_0 . The gradients α calculated for displacement less than about 6 cm are 0.106 kN^2/cm^3 for $PW-3$, 0.236 kN^2/cm^3 for $PW-5$ and 0.652 kN^2/cm^3 for $PW-10$. Substituting β and σ_n which is resultant from γ_i times depth z from surface into equation (9), the frictional coefficient can be estimated as amount of 0.409 for $PW-3$, 0.200 for $PW-5$ and 0.246 for $PW-10$, which corresponds to frictional angle of 22.2°, 11.3° and 13.8° respectively. These values are less than half that obtained from direct shear test.

Table 3 lists the estimated amounts of rigidities and frictional coefficients.

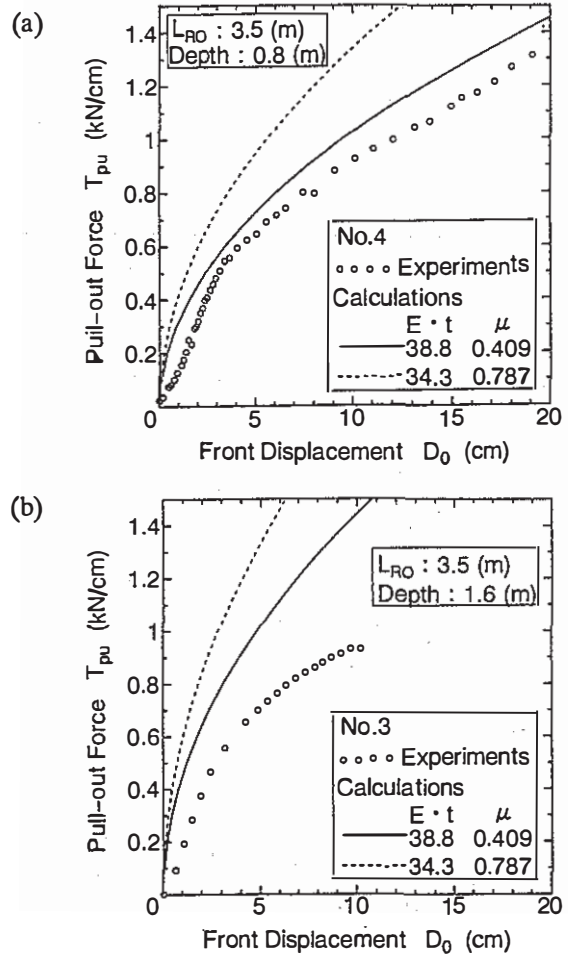


Fig. 10 Simulations of T_{pu} versus D_0 for $PW-3$ with embedment length of 3.5 m

In order to check practical utility of the estimated parameters, relationship between pull-out force and displacement at front end was simulated based on equation (6) for reinforcement with embedment length of 3.5 m.

Figs. 10(a),(b) and Figs. 11(a),(b) show the calculations and the experiments for $PW-3$ and $PW-5$ respectively. Relating to $PW-3$, the calculation in case of depth of 0.8 m is good agreement with the experiments. In case of depth of 1.6 m, however, displacement of the calculation is about half the experiment. It is considered for a reason that the experiment in case of depth of 1.6 m is almost the same as that in 0.8 m and therefore the confined pressure σ_n might be not so large as that calculated as $z \cdot \gamma_i$, especially near the vertical wall.

Relating to $PW-5$, the calculations simulate the trends of the experiments successfully while their displacements are somewhat less.

It is also pointed out that the calculations using the values from tensile test and direct shear test are remarkable under-estimate of displacement as seen in Figs. 10 and 11.

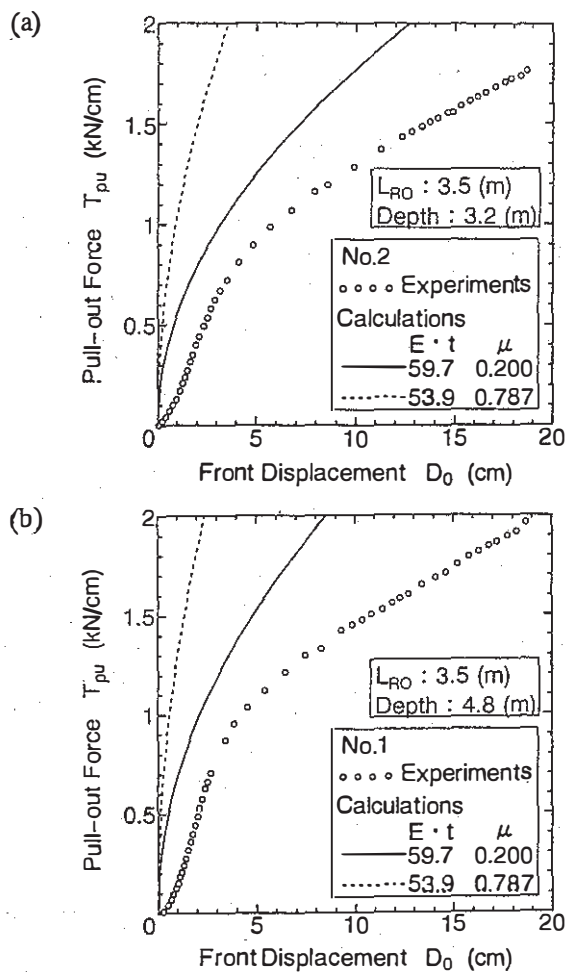


Fig. 11 Simulations of T_{pu} versus D_0 for PW-5 with embedment length of 3.5 m

5 CONCLUSIONS

An elastic relationship between pull-out force and displacement at front end was developed. The observation data obtained from field pull-out tests were analyzed based on derived formula to determine the rigidity and the frictional coefficient.

The followings are main conclusion;

- (1) Proposed formula relating pull-out force and displacement at front end can simulate well the observations.
- (2) Estimated rigidity $E \cdot t$ as a gradient of relation between pull-out force and creating strain at any position is good agreement with that obtained from tensile test.
- (3) Estimated frictional coefficient from a relation between square of pull-out force and displacement at front end is about half that obtained from direct shear test.

REFERENCES

- S.Hayashi, K.Makiuchi, H.Ochiai, M.Fukuoka and T.Hirai 1994. Testing Methods for Soil-Geosynthetic Friction at Geosynthetic Interfaces. *Proc. of the 5th International Conference on Geotextiles, Geomembranes and Related Products*. pp411-414, Singapore.
- R.M.Koerner 1994. *Designing with Geosynthetics -Third Edition*, Prentics Hall, New Jersey.
- T.Konami, K.Murayama, T.Eguchi, H.Murata and O.Yamamoto 1992. Design and Practice of Web Reinforced Soil Wall. *Recent Case Histories of Permanent Geosynthetic-Reinforced Soil Retaining Walls*. pp.243-246. Rotterdam:Balkema